Article

Novel Vaccine That Blunts Fentanyl Effects and Sequesters Ultrapotent Fentanyl Analogues

Rodell C. Barrientos, Eric W. Bow, Connor Whalen, Oscar B. Torres, Agnieszka Sulima, Zoltan Beck, Arthur E. Jacobson, Kenner C. Rice, and Gary R. Matyas*

Cite This: *Mol. Pharmaceutics* 2020, 17, 3447−3460

Read Online

ACCESS | 📊 Metrics & More | 📰 Article Recommendations | 🆘 Supporting Information

ABSTRACT: Active immunization is an emerging potential modality to combat fatal overdose amid the opioid epidemic. In this study, we described the design, synthesis, formulation, and animal testing of an efficacious vaccine against fentanyl. The vaccine formulation is composed of a novel fentanyl hapten conjugated to tetanus toxoid (TT) and adjuvanted with liposomes containing monophosphoryl lipid A adsorbed on aluminum hydroxide. The linker and hapten N-phenyl-N-(1-(4-(3-(tritylthio)propanamido)phenethyl)piperidin-4-yl)propionamide were conjugated sequentially to TT using amine-N-hydroxysuccinimide-ester and thiol−maleimide reaction chemistries, respectively. Conjugation was facile, efficient, and reproducible with a protein recovery of >98% and a hapten density of 30−35 per carrier protein molecule. In mice, immunization induced high and robust antibody endpoint titers in the order of >10^6 against the hapten. The antisera bound fentanyl, carfentanil, cyclopropyl fentanyl, *para*-fluorofentanyl, and furanyl fentanyl *in vitro* with antibody-drug dissociation constants in the range of 0.36−4.66 nM. No cross-reactivity to naloxone, naltrexone, methadone, or buprenorphine was observed. *In vivo*, immunization shifted the antinociceptive dose−response curve of fentanyl to higher doses. Collectively, these preclinical results showcased the desired traits of a potential vaccine against fentanyl and demonstrated the feasibility of immunization to combat fentanyl-induced effects.

KEYWORDS: fentanyl, opioid vaccine, ALF, conjugate vaccine, fentanyl analogues
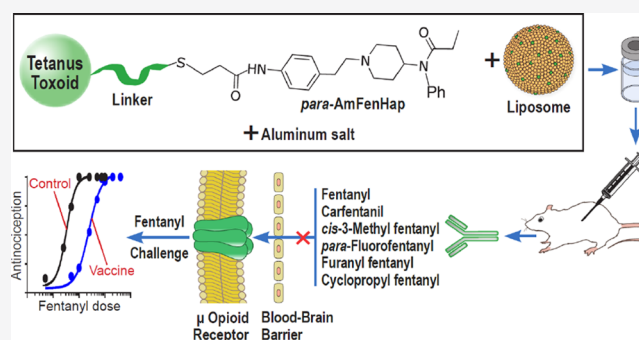
INTRODUCTION

Opioid use disorders and an epidemic of fatal overdose due to the illicit use of heroin and fentanyl are a growing concern worldwide.[1−4] In the United States alone, on average, 128 Americans die from opioid overdose each day.[5] Among the 46,802 deaths reported in 2018, 67% were due to synthetic opioids, mostly fentanyl and its analogues.[5] Fatal respiratory depression is the primary hazard of these compounds.[6,7] Fentanyl (Figure 1A) is 35−50× more potent as an analgesic than heroin.[6] Because of its potency, ease of manufacturing, and low cost, fentanyl has been used to lace other illicit substances of abuse. Deaths due to fentanyl-laced illegal drugs—heroin, cocaine, hydrocodone, and others—have been increasing over the years.[8] Alarmingly, highly potent fentanyl analogues such as carfentanil, cyclopropyl fentanyl, (±)-*cis*-3-methyl fentanyl, and furanyl fentanyl have been used as adulterants in illicit drugs, which have resulted in many fatal overdose cases.[8−10] The more potent fentanyl analogues, for example, carfentanil, could pose a risk to national security because of its potential use as a chemical weapon.[11,12] The abuse of fentanyl and other opioids has also been shown to be one of the causes of the spread of human immunodeficiency virus (HIV),[13] hepatitis C virus (HCV), and other infectious
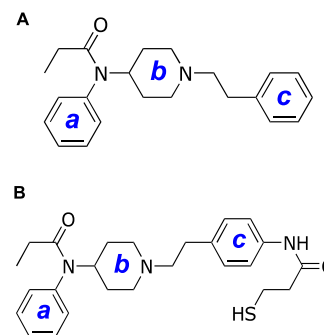

Figure 1. Structure of fentanyl (A) and hapten N-phenyl-N-(1-(4-(3-(tritylthio)propanamido)phenethyl)piperidin-4-yl)propionamide (*para*-AmFenHap) (B) described in this study. The labels *a* (for the anilido-ring), *b* (for the piperidine ring), and *c* (for the phenyl in the phenethyl moiety) are used throughout the article to refer to these parts of the fentanyl molecule.

diseases.[14,15] Among the 1.8 million HIV cases reported in 2018 in the United States, 125,000 were attributed to injection drug use.[16] Finally, the opioid epidemic has incurred a tremendous economic burden with an estimated annual cost of ~$7.8 billion in the United States[17] which underscores the need to develop new, practical, and sustainable strategies to address fentanyl overdose cases and to mitigate opioid use disorders.

Available clinical interventions to manage opioid addiction and to rescue fatal overdose—such as opioid management therapy and naloxone—remain limited. Opioid management therapy,[18] which uses naltrexone, methadone, and buprenorphine, alone or in conjunction with naloxone while effective, is impeded by issues of patient adherence rates and access to treatment facilities.[19,20] Individuals enrolled in these treatment modalities who suddenly halt or begin tapering of treatment medications are typically involved in opioid overdose.[20] Naloxone, a μ opioid receptor antagonist sold under the trade name NARCAN and EZVIO remains the gold standard rescue drug.[21] Naloxone displaces receptor-bound opioids in the brain to attenuate opioid-induced effects; however, multiple doses may be required to reverse the effects of synthetic fentanyl analogues.[21,22] In overdose scenarios, naloxone is most effective if given to victims shortly after being found unconscious, which may not always be practical. Additionally, naloxone precipitates opioid withdrawal symptoms and other complications.[21,23] Thus, current efforts are geared to develop practical alternatives or complementary modalities to naloxone. A long-lasting prophylactic vaccine that induces antibodies that impede brain access of fentanyl and its analogues is one such strategy.

Active immunization is an emerging approach that might be useful as a medication for opioid use disorders.[2,24−26] Immunization induces an immune response against the opioid immunogen, and the antibodies produced can sequester these drugs in the blood.[24,25] This impedes the ability of opioids to permeate the blood−brain barrier and prevent their access to receptors in the brain. Opioids alone are not immunogenic owing to their small molecular size.[25,27] To induce an immune response against these drugs, proxy molecules of the original opioid, otherwise called haptens, are attached to a carrier protein and are presented to the immune system in a T-cell-dependent manner.[25] Vaccines designed against nicotine,[28] methamphetamines,[29] cocaine,[30] oxycodone,[31] heroin,[32] and fentanyl[33−38] used the same approach. Stoichiometrically, a vaccine is most effective when the antibody concentration is high.[39] Because fentanyl is very potent, only small doses are required to induce toxic effects, suggesting that immunization could be a viable strategy to block fentanyl overdose.[36,37]

In this study, we report a novel and practical vaccine formulation that blocks fentanyl-induced effects in mice. The antigen contained the hapten (*para*-AmFenHap) (Figure 1B) that is conjugated to tetanus toxoid (TT) carrier protein. This antigen was coformulated with an adjuvant formulation composed of army liposome formulation (ALF) with monophosphoryl lipid A and 43% cholesterol, otherwise called ALF43,[40−42] and adsorbed on Alhydrogel (ALF43A). To test this formulation, we immunized mice with TT−*para*-AmFenHap/ALF43A vaccine and evaluated immunogenicity and efficacy. We found that the vaccine induced high-affinity antibodies against fentanyl and its highly potent analogues and protected mice against fentanyl-induced antinociceptive effects. These results demonstrated the feasibility of a practical vaccine

against fentanyl that warrants further development for clinical testing.

■ MATERIALS AND METHODS

General Methods, Key Materials, and Reagents. All melting points were determined on a Thomas-Hoover melting point apparatus or a Mettler Toledo MP70 system and are uncorrected. Proton and carbon nuclear magnetic resonance (^{1}H and ^{13}C NMR) spectra were recorded on a Varian Gemini-400 spectrometer in CDCl$_3$ (unless otherwise noted) with the values given in ppm (trimethylsilane, as the internal standard) and J (Hz) assignments of ^{1}H resonance coupling. High-resolution mass spectra (HRMS) were recorded on a VG 7070E spectrometer or a JEOL SX102a mass spectrometer. Thin-layer chromatography (TLC) analyses were carried out on Analtech silica gel GHLF 0.25 mm plates using 10% NH$_4$OH/CH$_3$OH in CHCl$_3$ or ethyl acetate (EtOAc) in hexanes. Visualization was accomplished under UV light (254 nm) or by staining in an iodine chamber. Flash column chromatography was performed using RediSep Rf normal phase silica gel cartridges. Robertson Microlit Analytical Laboratories, Ledgewood, NJ 07852 performed elemental analyses, and the results were within ±0.4% of the theoretical values.

The NHS−(PEG)$_2$−maleimide cross-linker [succinimidyl-[(N-maleimidopropionamido)-diethylene glycol]ester, SM-(PEG)$_2$], spin desalting columns (Zeba, 7k MWCO), dialysis cassettes (Slide-A-Lyzer G2, 10k MWCO), Pierce bicinchoninic acid (BCA) protein assay kit, and the bovine serum albumin (BSA) that was used for coupling reactions were purchased from Fisher Scientific (Rockford, IL). TT was purchased from MassBiologics (Mattapan, MA). Dulbecco's phosphate-buffered saline (DPBS, pH 7.4) was purchased from Quality Biological Inc. (Gaithersburg, MD). Lipids used to prepare liposomal adjuvant, 1,2-dimyristoyl-*sn*-glycero-3-phosphoglycerol (DMPG), 1,2-dimyristoyl-*sn*-glycero-3-phosphocholine (DMPC), monophosphoryl 3-deacyl lipid A (3D-PHAD) (MPLA), and cholesterol were purchased from Avanti Polar Lipids (Alabaster, AL), and Alhydrogel was purchased from Brenntag (Reading, PA). The list of materials and reagents used for the deprotection of hapten, enzyme-linked immunosorbent assay (ELISA), and liquid chromatography−tandem mass spectrometry (LC−MS/MS) are provided in Methods in the Supporting Information.

Hapten Synthesis. 2-(4-Nitrophenyl)-1-(4-(phenylamino)piperidin-1-yl)ethan-1-one (**1**) was synthesized following a previously published procedure.[43]

1-(4-Nitrophenethyl)-N-phenylpiperidin-4-amine (2). To a solution of **1** (50.0 mmol, 17.0 g) in anhydrous tetrahydrofuran (THF) (200 mL) was added a 1 M solution of BH$_3$ in THF (150 mmol, 150 mL), and the reaction was heated to reflux. After 1.5 h, the reaction was slowly quenched with CH$_3$OH and concentrated under vacuum. The resultant residue was suspended in 1 N HCl and refluxed for 3 h, then cooled to 0 °C and basified to *ca.* pH 9.0 with 28% NH$_4$OH, extracted with CHCl$_3$ (3 × 100 mL), dried over Na$_2$SO$_4$, and concentrated under vacuum. The residual oil was taken up in CHCl$_3$, and the mixture was brought to reflux. Approximately two-thirds of the solvent were removed by distillation and an equal volume of isopropanol was charged. The distillation was continued until the vapor temperature reached 80 °C. The solution was cooled to room temperature and stirred for 2 h and then filtered to collect the product as orange crystals (10.9

g, 67%), mp 92−94 °C. ^{1}H NMR (400 MHz; CDCl$_3$): δ 8.17 (d, J = 8.4 Hz, 2H), 7.41 (d, J = 8.3 Hz, 2H), 7.15 (t, J = 7.7 Hz, 2H), 6.69 (t, J = 7.3 Hz, 1H), 6.56 (d, J = 8.0 Hz, 2H), 4.46 (d, J = 13.7 Hz, 1H), 3.82 (d, J = 7.4 Hz, 3H), 3.51−3.46 (m, 2H), 3.19 (t, J = 12.5 Hz, 1H), 2.91 (t, J = 12.4 Hz, 1H), 2.05 (t, J = 12.7 Hz, 2H), 1.37−1.28 (m, 1H), 1.23−1.14 (m, 1H). ^{13}C NMR (101 MHz; CDCl$_3$): δ 167.77, 146.94, 146.39, 142.68, 129.83, 129.38, 123.81, 117.77, 113.26, 49.73, 44.83, 40.91, 40.41, 32.73, 32.05.

N-(1-(4-Nitrophenethyl)piperidin-4-yl)-N-phenylpropiona-mide (3). To a solution of **2** (3.07 mmol, 1.0 g) in anhydrous acetonitrile (ACN) (30 mL) was added K$_2$CO$_3$ (6.15 mmol, 0.85 g), followed by propionyl chloride (3.38 mmol, 0.3 mL). After 2 h, the reaction was quenched with H$_2$O and extracted with CHCl$_3$ (3 × 25 mL), dried over Na$_2$SO$_4$, and concentrated under vacuum. The crude residue was dissolved in hot cyclohexane and allowed to slowly cool to room temperature, stirred for 1 h, and then filtered to collect the product as white crystals (0.89 g, 76% yield), mp 120−122 °C. ^{1}H NMR (400 MHz; CDCl$_3$): δ 8.08 (d, J = 8.4 Hz, 2H), 7.39−7.34 (m, 3H), 7.27 (d, J = 8.4 Hz, 2H), 7.05 (d, J = 6.9 Hz, 2H), 4.65 (t, J = 12.2 Hz, 1H), 2.93 (d, J = 11.3 Hz, 2H), 2.79 (t, J = 7.9 Hz, 2H), 2.53 (t, J = 8.0 Hz, 2H), 2.15 (t, J = 11.6 Hz, 2H), 1.90 (q, J = 7.4 Hz, 2H), 1.78 (d, J = 11.8 Hz, 2H), 1.41−1.33 (m, 2H), 0.98 (t, J = 7.4 Hz, 3H). ^{13}C NMR (101 MHz; CDCl$_3$): δ 173.51, 148.21, 146.43, 138.77, 130.34, 129.39, 129.27, 128.27, 123.57, 59.43, 53.04, 52.03, 33.64, 30.51, 28.48, 9.56.

N-(1-(4-Aminophenethyl)piperidin-4-yl)-N-phenylpropio-namide (4). A solution of **3** (0.66 mmol, 250 mg) in ethanol (EtOH) (15 mL) was transferred to a pressure bottle, Escat 103 (5% Pd/C, 0.05 g) was added, and the bottle was pressurized to 50 psi H$_2$ in a Parr shaker. After 2 h, the reaction was filtered through celite and concentrated under vacuum. The product **4** was obtained as a hydrochloride salt (84 mg, 33%) following the literature procedure.[43] ^{1}H NMR (400 MHz; CDCl$_3$): δ 7.35 (q, J = 7.4 Hz, 3H), 7.05 (d, J = 7.0 Hz, 2H), 6.91 (d, J = 8.0 Hz, 2H), 6.57 (d, J = 8.0 Hz, 2H), 4.69−4.62 (m, 1H), 4.64 (t, J = 0.7 Hz), 3.52 (s, 2H), 2.96 (d, J = 11.4 Hz, 2H), 2.59 (dd, J = 10.4, 6.0 Hz, 2H), 2.44 (dd, J = 10.9, 5.5 Hz, 2H), 2.11 (t, J = 11.7 Hz, 2H), 1.90 (q, J = 7.4 Hz, 2H), 1.77 (d, J = 11.9 Hz, 2H), 1.44−1.35 (m, 2H), 0.99 (t, J = 7.4 Hz, 3H). ^{13}C NMR (101 MHz; CDCl$_3$): δ 173.47, 144.39, 138.81, 130.40, 130.15, 129.35, 129.22, 128.19, 115.20, 60.85, 53.08, 52.13, 32.92, 30.54, 28.49, 9.59.

N-Phenyl-N-(1-(4-(3-(tritylthio)propanamido)phenethyl)-piperidin-4-yl)propionamide (5). To a solution of **4** (140 mg, 0.4 mmol) in anhydrous dichloromethane (DCM) (10 mL) were added 2-(1*H*-benzotriazol-1-yl)-1,1,3,3-tetramethylami-nium tetrafluoroborate (TBTU) (1.2 mmol, 385 mg), 3-(tritylthio)propionic acid (1.2 mmol, 418 mg), and triethyl-amine (1.6 mmol, 0.22 mL). After 24 h, the reaction was quenched with H$_2$O and extracted with DCM (3 × 10 mL), dried over Na$_2$SO$_4$, and concentrated under vacuum. Purification via flash column chromatography on silica gel (isocratic, 50:49:1 DCM/ACN/28% NH$_4$OH) gave the product as a white foam (132 mg, 47%). ^{1}H NMR (400 MHz; CDCl$_3$): δ 7.42−7.30 (m, 10H), 7.26 (t, J = 7.8 Hz, 6H), 7.19 (t, J = 7.1 Hz, 3H), 7.10−7.03 (m, 5H), 4.64 (t, J = 12.1 Hz, 1H), 2.93 (d, J = 11.0 Hz, 2H), 2.64 (t, J = 8.0 Hz, 2H), 2.55 (t, J = 7.2 Hz, 2H), 2.45 (dd, J = 10.3, 5.8 Hz, 2H), 2.14−2.06 (m, 4H), 1.90 (q, J = 7.4 Hz, 2H), 1.76 (d, J = 12.0 Hz, 2H), 1.67 (s, 1H), 1.38 (q, J = 11.0 Hz, 2H), 0.99 (t, J =

7.4 Hz, 3H). ^{13}C NMR (101 MHz; CDCl$_3$): δ 173.55, 173.55, 169.05, 169.05, 144.56, 144.56, 138.73, 138.73, 136.19, 136.19, 135.71, 135.71, 130.37, 130.37, 129.54, 129.54, 129.25, 129.25, 129.01, 129.01, 128.24, 128.24, 127.94, 127.94, 126.70, 126.70, 119.88, 119.88, 60.42, 60.42, 53.03, 53.03, 52.10, 52.10, 36.69, 36.69, 33.17, 33.17, 30.52, 30.52, 28.51, 28.51, 27.65, 27.65, 9.61. HRMS (TOF MS ESI$^+$) calcd for C$_{44}$H$_{47}$N$_3$O$_2$S (M + H$^+$): 682.3467; found 682.3475. Calcd for C$_{44}$H$_{47}$N$_3$O$_2$S·0.47 CHCl$_3$: C, 71.38; H, 6.39; N, 5.60; found: C, 71.37; H, 6.46; N, 5.62.

Deprotection of Hapten. Trityl-capped *para*-AmFenHap was deprotected as described.[44] Briefly, trityl-capped *para*-AmFenHap (12 mg) was solubilized in chloroform (1.5 mL), treated with trifluoroacetic acid (150 μL) and triethylsilane (75 μL) for 1 h at room temperature, and concentrated under vacuum overnight. The residue was washed with petroleum ether and evaporated to dryness under vacuum. The residue was reconstituted in dimethyl sulfoxide (DMSO) (1 mL) and used for subsequent conjugation.

Hapten Conjugation to TT. A reaction based on thiol−maleimide chemistry[44,45] was used to conjugate *para*-AmFenHap to TT. Briefly, surface amino groups in TT (1 mg/mL stock) were activated by reacting with a solution of 250 mM SM(PEG)$_2$ in DMSO at a protein/linker ratio of 1:1600 for 2 h at 25 °C in BupH 7.2 (100 mM sodium phosphate, 150 mM sodium chloride, pH 7.2). Excess linker was removed by a spin column (Zeba, 7k MWCO), and the flow through containing TT−maleimide was reacted with deprotected *para*-AmFenHap at a protein/hapten molar ratio of 1:300 for 2 h at 25 °C in BupH 7.2. Before being used for conjugation, the hapten concentration was measured by Ellman's assay, where ~20−30 mM was obtained (Methods in the Supporting Information).[44] The reaction products were transferred to dialysis cassettes (Slide-A-Lyzer G2, 10k MWCO) and repeatedly dialyzed overnight against DPBS, pH 7.4 at 4 °C. Protein concentration was quantified using Pierce BCA assay kit following manufacturer's instructions.

Determination of Hapten Density. Hapten density was quantified by matrix-assisted laser desorption/ionization time-of-flight MS (MALDI-TOF MS), as described previously.[32,44] Briefly, unconjugated TT, unconjugated BSA, TT−*para*-AmFenHap, and BSA−*para*-AmFenHap were desalted using C4 ZipTip. Samples (0.5 μL) were mixed with (0.5 μL) sinapinic acid (10 mg/mL) in 50:50 ACN/H$_2$O 0.1% formic acid (FA) and spotted on a MALDI-TOF 384-well stainless plate and loaded to the AXIMA MegaTOF instrument (Shimadzu Scientific Instruments, Columbia, MD). The instrument was calibrated using either IgG (for samples containing TT) or BSA (for samples containing BSA). MS were acquired using the following settings: tuning mode, linear; laser power, 60−70; profiles, 500; shots, 2 per profile. Spectra were smoothed using the Gaussian method, and masses were assigned using threshold apex peak detection method. The number of the haptens attached per TT molecule was calculated using eq 1

$$\text{hapten density} = \frac{\text{mass}_{\text{protein−hapten conjugate}} - \text{mass}_{\text{unconjugated protein}}}{\text{mass}_{\text{linker+hapten}}}$$

(1)

The net addition mass for linker + hapten, mass$_{\text{linker+hapten}}$ = 749.74 g/mol.

Vaccine Formulation. The final vaccine formulation (50 μL) was composed of 10 μg of TT−*para*-AmFenHap (based

on the protein content of the protein−hapten conjugate), 20 μg of synthetic monophosphoryl 3-deacyl lipid A (3D-PHAD) in ALF43, and 30 μg of aluminum in aluminum hydroxide (Alhydrogel) in DPBS pH 7.4. ALF43 contained DMPC/DMPG/cholesterol/3D-PHAD at a molar ratio of 9:1:7.5:1.136; the molar ratio of phospholipids/3D-PHAD was 8.8:1. ALF43, derived from small unilamellar vesicles, was prepared as lyophilized powder following the detailed procedures as previously described.[41,42,46] The total concentration of phospholipids in the reconstituted ALF43A was 2.29 mM.

Animal Studies. All animal studies were conducted under an approved animal use protocol in an Association for Assessment and Accreditation of Laboratory Animal Care International (AAALACi)-accredited facility in compliance with the Animal Welfare Act and other federal statutes and regulations relating to animals. Experiments involving animals adhered to the principles stated in the Guide for the Care and Use of Laboratory Animals, 8th edition.[47] Briefly, ~7-week-old female BALB/c mice (n = 10 control and n = 10 vaccine group) (Jackson Laboratories, Bar Harbor, ME) were immunized *via* intramuscular (i.m.) route at alternate rear thighs with 50 μL of vaccine formulation on weeks 0, 3, 6, and 14. Challenge experiments were performed at week 18 *via* a subcutaneous (s.c.) route using fentanyl·HCl in 0.9% saline (0.0050 to 4.0 mg/kg). This route has been used previously to evaluate anti-fentanyl vaccines.[36,37] Control mice did not receive any vaccination. Antinociceptive effects were assessed 15 min after each fentanyl injection.

Nociception Assays. Two nociception assays, tail immersion and hot plate, were used to evaluate vaccine efficacy.[48,49] In the tail-immersion assay, the mouse tail was immersed in a water bath set at 54 °C (IITC Life Science, Woodland Hills, CA). The latency times were measured with a cutoff time of 8 s to prevent tail injury. Antinociception, measured as % maximum potential effect (% MPE), was calculated using eq 2

$$\% \text{ MPE} = \frac{\text{post fentanyl injection latency time} - \text{baseline latency time}}{\text{cutoff latency} - \text{baseline latency time}} \times 100 \tag{2}$$

In the hot plate assay, the mouse was placed on a hot plate analgesia meter (Harvard Apparatus, Holliston, MA) set at 54 °C and the latency time to show a nociceptive response with hind paw lick or a jump was measured.[49] If no response was observed within 30 s, the mouse was removed from the heated plate to prevent any tissue damage. Antinociception, measured as % MPE, was calculated from eq 2.

Enzyme-Linked Immunosorbent Assay. To assess immunogenicity, ELISA against BSA−*para*-AmFenHap was performed on sera collected at different time points (Figure 3A). The use of BSA−*para*-AmFenHap ensured the selectivity of the measured antibodies against the hapten and not against the carrier protein, TT.[25] Synthesis of the BSA−*para*-AmFenHap coating antigen is described in the Supporting Information Methods. Nunc Maxisorb flat-bottom plates were coated with BSA−*para*-AmFenHap antigen (0.1 μg/0.1 mL/well in DPBS), and the remainder of the procedure was performed as described previously.[42,48] Briefly, the plates were blocked with blocker (1% BSA in 20 mM Tris−0.15 M NaCl, pH 7.4) for 2 h. Mouse sera were serially diluted in blocker and added to the plates in triplicate. A mouse anti-fentanyl monoclonal antibody was used as a positive control. After

incubation for 2 h at room temperature, plates were washed with 20 mM Tris−0.15 M NaCl−0.05% Tween 20. Peroxidase linked-sheep anti-mouse IgG diluted in blocker (1:1000) was added, and the plates were incubated for 1 h at room temperature. The plates were washed and 2,2′-azino-bis(3-ethylbenzothiazoline-6-sulfonic acid) peroxidase substrate system (100 μL/well) was added. After incubation at room temperature for 1 h, the absorbance was measured at 405 nm.

Serum Binding Measurements. Serum binding was measured using equilibrium dialysis (ED), as described previously.[50] Mouse sera from week 16 were diluted with 0.05% BSA in DPBS, pH 7.4 (ED buffer) containing 5 nM of a drug. An aliquot (100 μL) was seeded into sample chambers of rapid ED plate, and the buffer chamber was filled with 300 μL of ED buffer. The plate was incubated at 4 °C and 300 rpm for 24 h in a thermomixer. Aliquots (90 μL) from sample and buffer chambers were pipetted out, spiked with 1 μL of 10% FA, and analyzed by LC−MS/MS.

Determination of Antibody Affinity (K_d) and Relative Antibody Binding Site Concentration. The K_d of anti-hapten antibodies in serum was measured using competition ED as noted.[50] Briefly, mouse sera were diluted with 5 nM of isotopically labeled tracer drug (d_x where x = 3, 5, or 6 heavy isotopes) in ED buffer at a serum dilution that yielded 50% binding in the serum binding experiments. The buffer chambers were filled with ED buffer that contains an increasing concentration of competitor drug (final concentration, 0 to 40 nM). Half maximal inhibitory concentration (IC$_{50}$) was interpolated using four-parameter logistic curve (plot of % inhibition vs concentration of the competitive inhibitor). The % inhibition values were obtained using eq 3 and were used to calculate K_d according to eq 4[50]

$$\% \text{ inhibition} = 100 \times \left(1 - \frac{[d_x]_{\text{bound},I}}{[d_x]_{\text{bound},I_0}}\right) \tag{3}$$

where $[d_x]_{\text{bound},I} = [d_x]_{\text{sample chamber}} - [d_x]_{\text{buffer chamber}}$. $[d_x]_{\text{bound},I_0}$ = concentration of the d_x-tracer in the absence of the competitive inhibitor

$$K_d = ([I_{50}] - [T_t])(1 - 1.5b + 0.5b^2) \tag{4}$$

where $[I_{50}]$ = molar concentration of the competitive inhibitor required for 50% inhibition. $[T_t]$ = total molar concentration of d_x-tracer after equilibrium (typical value is 1.25 nM). b = fraction of bound d_x-tracer in the absence of the competitive inhibitor.

Antibody binding site concentration [Ab] was calculated using eq 5[51]

$$[\text{Ab}] = \left[b[T_t] + \frac{bK_d}{(1 - b)}\right]f \tag{5}$$

where [Ab] = relative antibody binding site concentration (nM). b = fraction of bound d_x-tracer in the absence of the competitive inhibitor. $[T_t]$ = total molar concentration of d_x-tracer after equilibrium (typical value is 1.25 nM). K_d = dissociation constant (nM). f = serum dilution factor.

Liquid Chromatography−Tandem Mass Spectrometry. A binary ultraperformance liquid chromatograph (UPLC) (Waters, Milford, MA) coupled with a triple quadrupole detector (Waters, Milford, MA) was used to quantify the concentration of drugs from ED experiments as reported previously with minor modifications.[50] An ACQUITY HSS T3

Scheme 1. Synthesis of Trityl-Protected Hapten *para*-AmFenHap (5)[a]
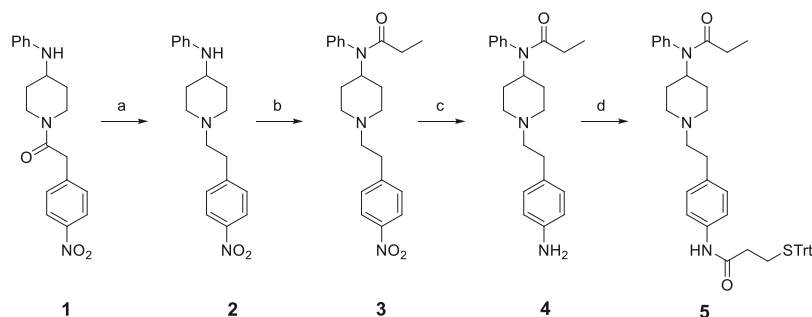
[a]Reagents and conditions: (a) BH_3, THF, 65 °C, 1.5 h, 67%; (b) K_2CO_3, propionyl chloride, ACN, 2 h, 76%; (c) H_2, 5% Pd/C, EtOH, 2 h, 33%; (d) 3-(tritylthio)propionic acid, TBTU, triethylamine, DCM, 24 h, 47%.

column (2.1 × 100 mm, 1.8 μm particle size) (Waters, Milford, MA) and the following mobile phases were used: A (10 mM NH_4COOH with 0.1% FA), B (MeOH with 0.1% FA). The UPLC gradient used is provided in Supporting Information Table S1. The column was maintained at 65 °C at a flow rate of 500 μL/min. The injection volume was 10 μL using a full-loop injection mode. To avoid carryover, the autosampler needle was rinsed with a weak wash (600 μL, 10% MeOH in H_2O) and a strong wash (200 μL, 90% ACN in H_2O) before each injection.

All data were acquired using positive electrospray ionization (ESI) in the multiple reaction monitoring (MRM) mode. The electrospray and source settings were as follows: 0.7 kV (capillary voltage), 120 °C (source temperature), 500 °C (desolvation temperature), 900 L/h (desolvation gas flow, N_2), and 60 L/h (cone gas flow, N_2). The collision gas (Ar) flow in the collision cell was maintained at 0.3 mL/min. MRM transitions are provided in Supporting Information Table S2. Data were processed using external calibration with $1/X^2$ weighting in TargetLynx application of MassLynx version 4.2 software (Waters, Milford, MA).

Data Analysis. The 3D molecular modeling of compounds described in this study was performed in ChemDraw 19.1. Structures were energy minimized using the built-in molecular mechanics 2 (MM2) method. Data processing and analyses were performed using Prism 8 (GraphPad Inc., San Diego, CA). In competition, ED LC−MS/MS, IC_{50} was interpolated from the linear regression of % inhibition as a function of log-transformed concentrations of the competitive inhibitor. Statistical comparisons between the control and the TT−*para*-AmFenHap immunized group employed a two-tailed, unpaired Mann−Whitney U, nonparametric t-test. In comparing serum binding data, a two-tailed, paired t-test was used. The 50% effective dose (ED_{50}) values were interpolated from log-dose−response curves fitted using a four-parameter logistic nonlinear regression method. The difference between fentanyl dose−effect curves of control and vaccine was determined using global curve-fitting analysis (shared four parameters: top, bottom, hill slope, and ED_{50}) to calculate the global sum of squares.[52] The sums of squares of control and vaccine modeled using two separate curves were compared to the sums of squares from globally fitted curve to calculate the F statistic and p value. Statistical significance was defined as $p \leq 0.05$.

■ **RESULTS**

Hapten Synthesis and Conjugation to the Carrier Protein. The hapten *para*-AmFenHap (Figure 1B) is composed of the intact fentanyl scaffold, *N*-(1-phenethylpiperidin-4-yl)-*N*-phenylpropionamide, with a mercaptopropanamide moiety in the para position of the phenyl ring *c*. Synthesis of trityl-protected *para*-AmFenHap was accomplished in four steps, as shown in Scheme 1. The carbonyl **1** was first converted to **2** *via* borane−THF reduction (67% yield) followed by N-acylation with propionyl chloride to yield **3** (76% yield from **2**). The amino group in **4** was obtained by reducing the nitro group *via* hydrogenation using Pd/C as the catalyst (33% yield from **3**). Finally, the resultant amino group was coupled with 3-(tritylthio)propionic acid in the presence of TBTU to yield trityl-protected *para*-AmFenHap hapten (**5**) (47% yield from **4**).

Next, the antigen (Figure 2A) was synthesized by conjugating the hapten to TT−carrier protein through a two-step process. In the first step, surface amino groups were activated using $SM(PEG)_2$ to yield TT−maleimide. In the second step, TT−maleimide was conjugated with the trityl-deprotected hapten *via* thiol−maleimide chemistry (Figure 2B). The recovery of TT−*para*-AmFenHap was >98% based on protein content after the purification steps. The conjugate consistently gave a hapten density of 30−35 copies per carrier TT molecule, as quantified by MALDI-TOF MS (Supporting Information Figure S11).

Immunization Induces High Hapten-Specific Antibody Titers. To test the immunogenicity *in vivo*, female BALB/c mice ($n = 10$ per group) were immunized i.m. on alternate rear thighs on weeks 0, 3, 6, and 14 with 50 μL TT−*para*-AmFenHap/ALF43A vaccine formulation (Figure 3A). Serum antibody titers were measured using binding ELISA with BSA−*para*-AmFenHap as a coating antigen. We observed a gradual increase in antibody endpoint titers beginning at week 3 (Figure 3B). At week 16, the mean endpoint titers were 1, 820, 444, and 400 for immunized and unimmunized mice, respectively (Figure 3C). Antibodies against the carrier protein were also induced, albeit lower titer than that of the hapten (Supporting Information Figure S14).

Antisera from Immunized Mice Bind Fentanyl and Fentanyl Analogues *in Vitro*. The goal of immunization was to induce IgG that could act as a pharmacokinetic antagonist through sequestration of fentanyl in the blood. We tested the binding ability of vaccine-induced antibodies to fentanyl by ED followed by LC−MS/MS. To limit nonspecific binding and to permit multiple measurements from limited serum samples, sera were diluted subsequent to measurements.[50] This was acceptable, given that the endpoint titers measured were sufficiently high (*vide supra*). Preimmune (week 0) and
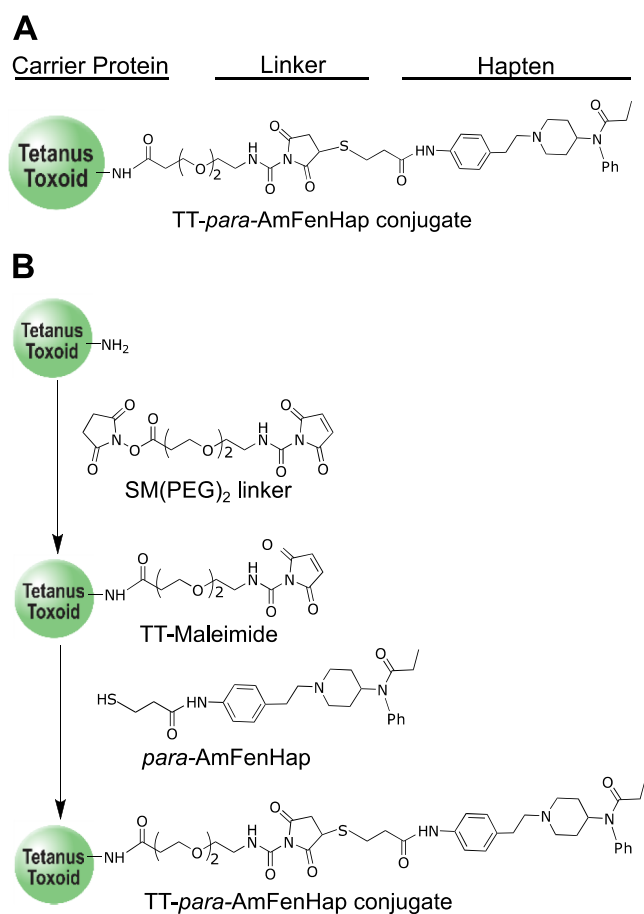
Figure 2. Antigen design, synthesis, and research strategy. (A) Design of the TT−*para*-AmFenHap antigen. (B) Synthesis scheme of TT−*para*-AmFenHap.

Figure 3. Immune response of the TT−*para*-AmFenHap vaccine to the hapten. Mice (n = 10/group) were immunized at weeks 0, 3, 6, and 14; and bled at weeks 0, 3, 6, 9, 14, and 16. Antibody titers were measured using binding ELISA with BSA−*para*-AmFenHap as a coating antigen. (A) Timeline of animal experiments. (B) IgG endpoint titers as a function of time. (C) IgG dilution curves for week 16 sera. Data shown are mean ± SD. Statistical comparisons (naïve control vs TT−*para*-AmFenHap) were performed using non-parametric Mann−Whitney U unpaired t-test (***, $p < 0.0005$).

postimmune (week 16) sera were diluted with 5 nM fentanyl in ED buffer and dialyzed against buffer for 24 h using a semipermeable membrane with 12 kDa MWCO. Dilutions were chosen such that 100% of the initial concentration of 5 nM fentanyl is bound (1:400 to 1:51,200). The amount of fentanyl in both sample and buffer chambers was quantified and used to determine fraction bound. Postimmune sera effectively bound fentanyl (fraction bound ≥ 0.60) even at very high serum dilution (1:6400) in contrast to preimmune sera (fraction bound < 0.25) in all dilutions tested (1:400 to 1:51,200) (Figure 4A).

We then tested the serum-binding property of fentanyl analogues carfentanil, cyclopropyl fentanyl, (±)-*cis*-3-methyl fentanyl, *para*-fluorofentanyl, and furanyl fentanyl. These were chosen because they have been among the most commonly seized fentanyl analogues by law enforcement within the last 5 years according to the U.S. National Forensic Laboratory Information System (NFLIS).[8] For ease of comparison with fentanyl, the analyses for all the compounds were performed at serum dilutions of 1:400 to 1:51,200, except for carfentanil, where the analysis was performed at serum dilutions of 1:200 to 1:6400. We found that the binding of all of the tested analogues was significantly higher in postimmune compared to preimmune sera (Figure 4). Analogues with modifications at the *N*-alkyl moiety (cyclopropyl fentanyl and furanyl fentanyl) had comparable postimmune sera binding with fentanyl (fraction bound ≥ 0.60 at dilutions 1:400 to 1:6400). However, those that have modifications in the piperidine
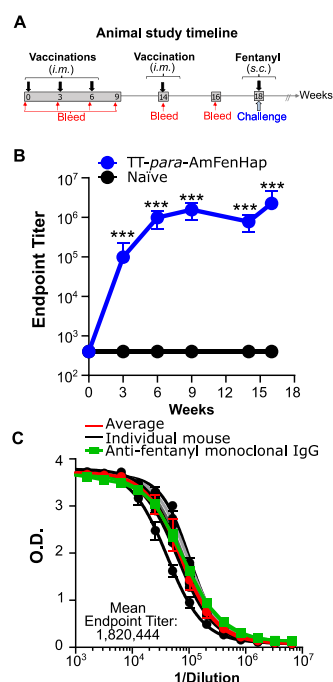
(*b*), and phenyl (*a*) rings showed lower fraction bound at the same sera dilution. Specifically, the analogues (±)-*cis*-3-methyl fentanyl, *para*-fluorofentanyl, and carfentanil had fraction bound values of ~0.25, ~0.50, and ~0.25, respectively, at 1:6400 dilution. We also tested norfentanyl (a metabolite of fentanyl that lacks the phenethyl group, i.e., ring *c*) and found that the fractions bound at 1:1600 to 1:6400 were less than those of fentanyl (Supporting Information Figure S15).

Antibodies Bind Fentanyl Analogues with High Affinity. Antibody affinity (K_d) measures the binding strength between IgG and its antigen. Using the competition ED−LC−MS/MS procedure published previously,[50] we measured the K_d values of fentanyl and selected fentanyl analogues. These values translated to nanomolar affinities following the order: cyclopropyl fentanyl (0.36 nM) ~ furanyl fentanyl (0.44 nM) ~ fentanyl (0.56 nM) > *para*-fluorofentanyl (1.16 nM) > carfentanil (4.66 nM) (Table 1). The IC_{50} data and inhibition curves used to calculate K_d values are provided in Supporting Information Table S3 and Figure S16.

We also calculated the relative antibody binding site concentrations for these analogues using the relationship between fraction bound at equilibrium and K_d values, as proposed by Müller.[51] The relative antibody binding site concentrations obtained were 13.83 ± 1.62 μM (fentanyl), 15.67 ± 1.08 μM (cyclopropyl fentanyl), 18.84 ± 1.60 μM (furanyl fentanyl), 12.99 ± 1.49 μM (*para*-fluorofentanyl), and 1.44 ± 0.18 μM (carfentanil). For the analogues (Figure 4D,E), the increasing *b* values obtained at 1:12,800, 1:25,600, and 1:51,200 were attributed to the normal variation of the assay especially for weakly binding drugs.[50] These values
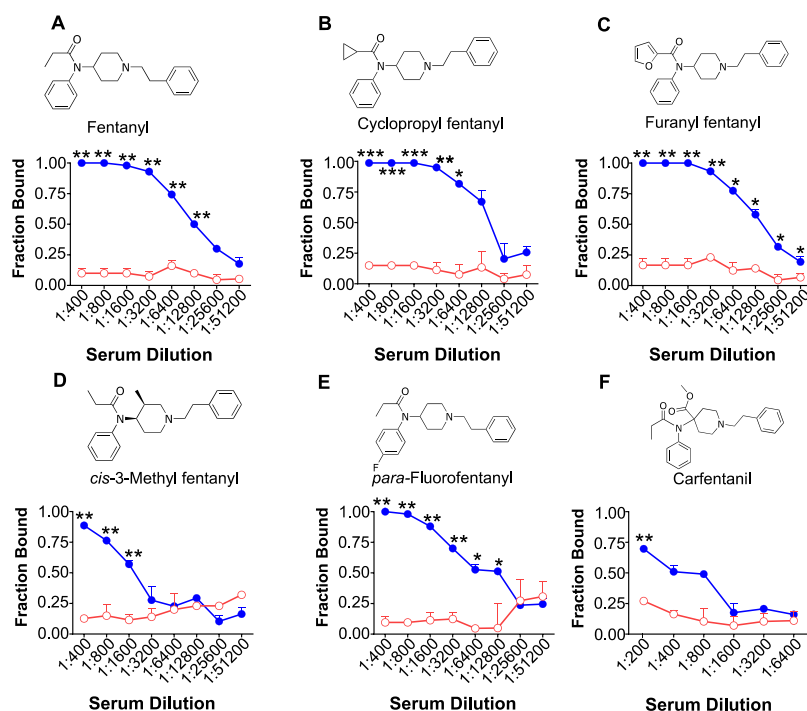
Figure 4. Serum binding of fentanyl and fentanyl analogues. Preimmune sera (week 0, red) and postimmune sera (week 16, blue) were diluted with a buffer that contained 5 nM of indicated drugs and dialyzed against buffer in an ED plate. Drug levels in the sample and buffer chambers were quantified after 24 h, and fraction bound was calculated. (A) Fentanyl. (B) Cyclopropyl fentanyl. (C) Furanyl fentanyl. (D) *cis*-3-Methyl fentanyl. (E) *para*-Fluorofentanyl. (F) Carfentanil. Data shown are mean ± standard error of the mean (SEM) of triplicate determinations. Statistical comparisons (preimmune vs postimmune sera) were performed using paired t-test (***, $p < 0.0001$; **, $p < 0.001$; *, $p < 0.010$; the absence of asterisk indicates that the difference is not significant).

Table 1. Antibody Affinity (K_d) and Relative Antibody Binding Site Concentrations ([Ab]) of Fentanyl and Selected Fentanyl Analogues *in Vitro* As Measured Using Competition ED−LC−MS/MS[a]

drug	K_d (nM)[b]	[Ab] (μM)[b]
fentanyl	0.56 ± 0.13	13.83 ± 1.62
cyclopropyl fentanyl	0.36 ± 0.06	15.67 ± 1.08
carfentanil	4.66 ± 0.67	1.44 ± 0.18
furanyl fentanyl	0.44 ± 0.08	18.84 ± 1.60
para-fluorofentanyl	1.16 ± 0.20	12.99 ± 1.49

[a]Using pooled, postimmune (week 16) sera. [b]Mean ± SD of triplicate determinations.

corroborate the serum binding results, where the weakly bound analogues (i.e., *para*-fluorofentanyl and carfentanil) had relatively lower antibody binding site concentrations. However, it must be noted that the binding site concentration is dependent on the K_d. Thus, it is most likely that the apparent reduced binding site concentration is actually the same binding site concentration with lesser binding affinity.

Mice Antisera Do Not Bind Opioid Abuse Pharmacotherapeutics. To determine if vaccine-induced antibodies can cross-react with drugs used for opioid abuse therapy, we tested serum binding against methadone, naltrexone, buprenorphine, and naloxone using ED−LC−MS/MS.[50] Binding to naloxone, methadone, buprenorphine, and naltrexone to postimmune sera was low (fraction bound <0.25) in all serum dilutions tested where fentanyl and fentanyl analogues were observed to bind (1:400 to 1:51,200). No difference was observed ($p > 0.05$) in postimmune and preimmune serum binding of

naloxone, methadone, buprenorphine, and naltrexone (Figure 5).

Immunization with TT−*para*-AmFenHap Attenuates Fentanyl Potency in Mice. We determined the efficacy of the vaccine to neutralize the antinociceptive effects of fentanyl in mice. Immunized and unimmunized mice were challenged s.c. on week 18 with increasing doses of fentanyl (0.0050 to 4.0 mg/kg). We assessed fentanyl effects by tail immersion and hot plate assays 15 min after each dosing and interpolated the ED_{50}. Full antinociceptive effects (100% MPE) of fentanyl were met at ~0.050 mg/kg for unimmunized mice and at ~1.00 mg/kg for immunized mice in both assays.

The statistical difference between fentanyl dose−effect curves of control and vaccine was determined using a global curve-fitting analysis to calculate the global sum of squares.[52] We found that fentanyl ED_{50} values shifted to higher doses in both assays (ED_{50} shifts: tail immersion = 4.3-fold, hot plate = 8.0-fold) (Figure 6). Specifically, in tail immersion, immunized mice had a fentanyl ED_{50} = 0.13 mg/kg [95% confidence interval (CI), 0.069−0.369] compared with naive mice which had a fentanyl ED_{50} of 0.03 mg/kg (95% CI, 0.014−0.043). These differences were found to be statistically significant [F = 24.78, degrees of freedom, numerator (DFn) = 4, degrees of freedom, denominator (DFd) = 136; $p < 0.0001$]. The ED_{50} values obtained in the hot plate assay were 0.24 mg/kg (95% CI, 0.179−0.313) and 0.03 mg/kg (95% CI, 0.025−0.040) for immunized and naive mice, respectively. These differences were also statistically significant (F = 284.26, DFn = 1, DFd = 172; $p < 0.0001$). Figure 6C shows the % MPE in hot plate nociception at relatively high doses of 0.050 and 0.10 mg/kg; immunized mice consistently had lower latency times in the hot plate assay.
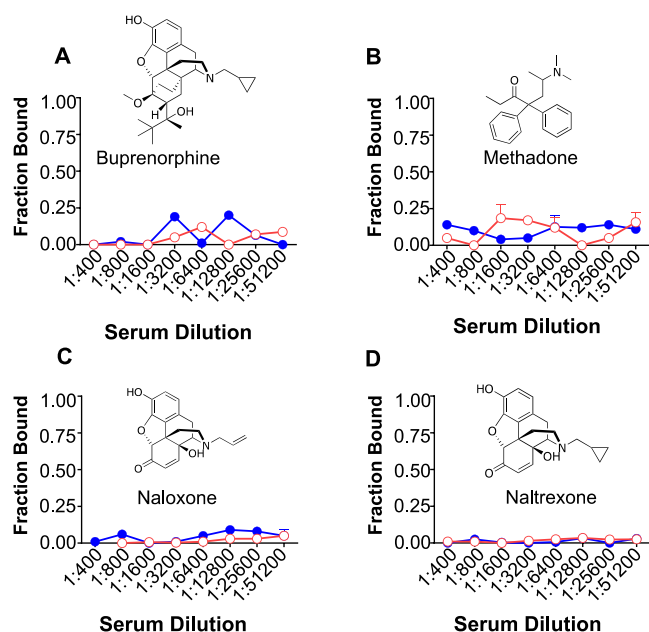
Figure 5. Serum binding of drugs used for opioid abuse therapy. Preimmune sera (week 0, red) and postimmune sera (week 16, blue) were diluted with a buffer that contained 5 nM of indicated drugs and dialyzed against buffer in an ED plate. Drug levels in the sample and buffer chambers were quantified after 24 h, and fraction bound was calculated. Data shown are mean ± SEM. No significant difference was observed in any of the dilutions shown (preimmune vs postimmune sera) using paired t-test.

■ DISCUSSION

Novel strategies are needed to combat opioid use disorders, particularly in the context of fentanyl abuse and overdose. Our present study addressed this public health burden by developing an efficacious vaccine against fentanyl that could neutralize both fentanyl and its highly potent analogues. Here, we presented the synthesis of a new fentanyl hapten, $para$-AmFenHap and its conjugation to TT carrier protein. We found that (1) TT–$para$-AmFenHap was highly immunogenic in mice as evidenced by high antibody titers against fentanyl hapten; (2) serum IgG in immunized mice bound fentanyl and fentanyl analogues (cyclopropyl fentanyl, carfentanil, furanyl fentanyl, $para$-fluorofentanyl, (±)-cis-3-methylfentanyl) but not drugs used for opioid abuse therapy (naloxone, naltrexone, methadone, or buprenorphine); and (3) immunization with TT–$para$-AmFenHap protected mice from antinociceptive effects of fentanyl.

The high immunogenicity of our vaccine can be attributed to the carrier protein and adjuvant components. Fentanyl is nonimmunogenic on its own, which requires conjugation to an immunogenic carrier protein and a potent adjuvant in order to induce an immune response. We conjugated $para$-AmFenHap to TT carrier protein, using the same method we used for a heroin vaccine;[32,45] we obtained equivalent yields and hapten density. We previously showed the superior immunogenicity of TT compared with other proteins in the context of a heroin vaccine.[32,46,48,53] Other groups have also showed the suitability of TT as carrier proteins in vaccines against other drugs of abuse such as fentanyl,[37] oxycodone,[54] and combination heroin–fentanyl.[55] We also showed that the use of the ALF43A adjuvant further enhanced its immunogenicity.[42] This is consistent with the results of this present study, where we
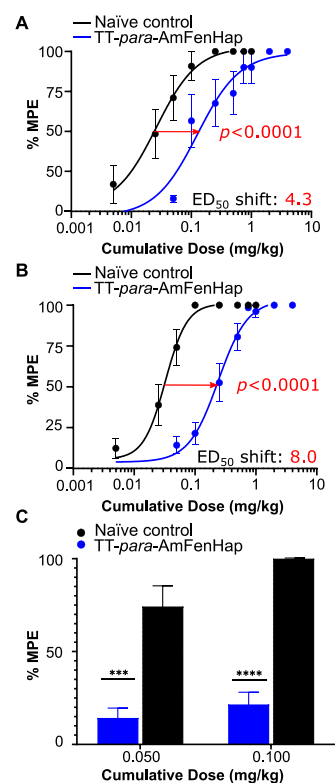

Figure 6. Vaccine efficacy against fentanyl-induced antinociception. On week 18, mice (n = 10/group) were challenged with increasing dose of fentanyl·HCl in 0.9% saline (0.0050 to 4.0 mg/kg) to establish dose–effect curves. Fentanyl-induced antinociceptive effects were evaluated using tail immersion and hot plate assays 15 min after each dose; results were reported as % MPE. (A) Tail-immersion antinociceptive effects. The ED_{50} values were control = 0.03 mg/kg (95% CI, 0.014–0.043) and TT–$para$-AmFenHap = 0.13 mg/kg (95% CI, 0.069–0.369) (F = 24.78, DFn = 4, DFd = 136; p < 0.0001). (B) Hot plate antinociceptive effects. The ED_{50} values were control = 0.03 mg/kg (95% CI, 0.025–0.040) and TT–$para$-AmFenHap = 0.24 mg/kg (95% CI, 0.179–0.313) (F = 284.26, DFn = 1, DFd = 172; p < 0.0001). (C) % MPE shown at cumulative doses of 0.050 and 0.100 mg/kg fentanyl from the hot plate assay curve in B. Shown are mean ± SEM. The difference between fentanyl dose–effect curves of control and vaccine was determined using a global curve-fitting analysis to calculate the F statistic and p value.[52] In (C), statistical comparisons vs control were performed using the unpaired Mann–Whitney U, nonparametric t-test, (****, p < 0.0001; ***, p < 0.001). CI, confidence interval; DFn, degrees of freedom, numerator; DFd, degrees of freedom, denominator.

observed reproducible high anti-hapten endpoint titers (Figure 3). TT is a Food and Drug Administration (FDA)-licensed vaccine component for tetanus and diphtheria toxin (TDVAX, MassBiologics),[56] while ALF43A is slated to be used in phase 1 HIV-1 vaccine clinical trial.[40] In addition, ALF43A had an acceptable safety profile when tested in rabbit repeat-dose toxicity studies. The conjugation procedure used here, along with the components of the current formulation, makes this a practical vaccine that could be easily translated to human trials.

In terms of the hapten design, the linker attachment site is important because it determines which face of the molecule is presented to the immune system; the latter eventually dictates the specificity of the induced IgG.[27,53] This is important for fentanyl vaccine design because the overarching goal is to produce an immune response against derivatives with varying degrees of structural features. A few fentanyl hapten designs
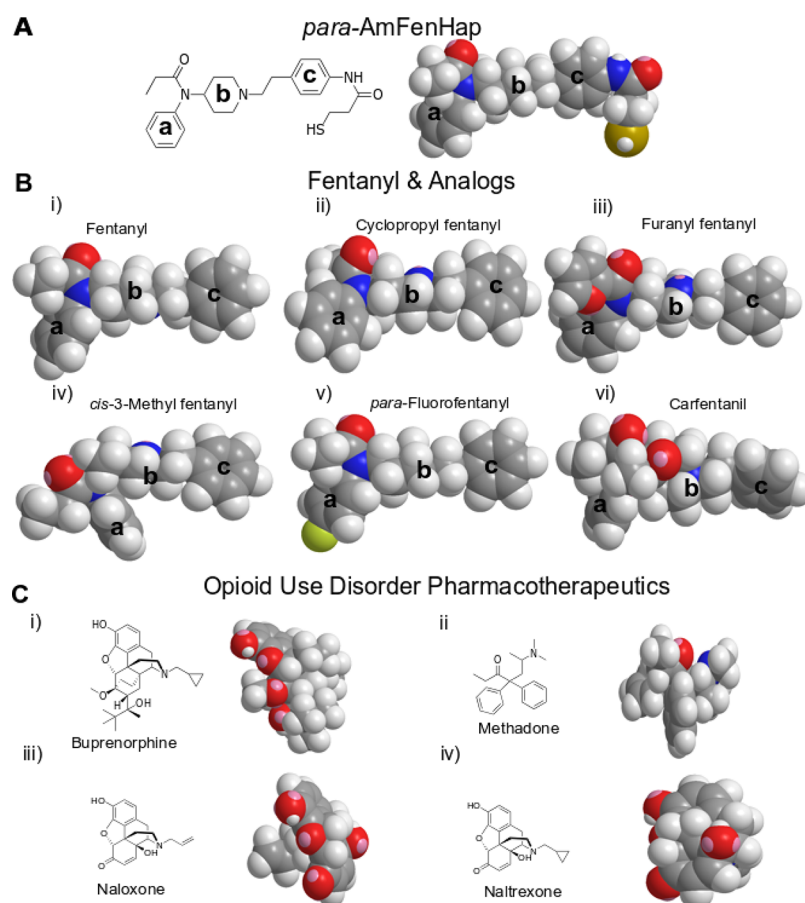
Figure 7. Space-filling models of *para*-AmFenHap and drugs used in serum binding experiments. (A) *para*-AmFenHap hapten; (B) fentanyl analogues; (C) drugs used for opioid use disorder therapy. The 3D structures were constructed in ChemDraw 19.1. The geometry and energy were optimized and minimized, respectively, using the built-in MM2 method.

have been reported previously, which were found to be efficacious in rats, mice, and nonhuman primates.[33,36,55,57] Specifically, Bremer et al.[37] reported a design, where the *N*-alkyl group served as a linker attachment site. Raleigh et al.[36] used a fentanyl surrogate, where the phenyl ring *c* was replaced with a linker. Our hapten uses the para-position of the terminal phenyl ring (ring *c*) as a linker attachment site. This allowed the presentation of intact fentanyl scaffold to the immune system and enabled the capture of small structural changes in the *N*-alkyl, phenyl, and piperidine moieties (Figure 7A), as reflected in the results of serum binding measurements.

In this study, we used two nociception assays, tail immersion and hot plate as a surrogate metric of vaccine efficacy.[25,49] These assays were used in order to assess the efficacy of the vaccine to attenuate fentanyl-induced effects in the centrally mediated (hot plate) and spinally mediated (tail immersion) nociception.[25,49,58] Immunization with TT–*para*-AmFenHap attenuated fentanyl-induced antinociception in both assays as evidenced by the ED_{50} shifts in immunized mice, which were 8-fold in hot plate and 4.3-fold in tail immersion, respectively. Previous reports on fentanyl vaccines also attenuated the potency of fentanyl in rodents.[36,37] Bremer et al.[37] reported ED_{50} shifts in the hot plate and tail flick assay of 24- and 33-fold, respectively, while Raleigh et al.[36] reported an ED_{50} shift of 5.4-fold in the hot plate assay. Together, these studies highlight the potential of active immunization to blunt fentanyl potency *in vivo*.

Opioid sequestration by IgG could be an effective approach to reduce the incidence of fatal overdose. By the law of mass action, high doses of drugs will require a higher concentration of neutralizing IgG, which may depend on antibody affinity.[59] This suggests that a more relevant metric of "effective" IgG concentration *in vivo* should account for the antibody-drug binding strength (i.e., K_d). We addressed this using eq 5 to calculate the drug-specific relative antibody binding site concentrations.[51] The fentanyl-specific relative antibody binding site was ~13.83 μM (Table 1). At this concentration, assuming a 25 g mouse with a total blood volume of ~2.0 mL, the maximum dose of fentanyl required to saturate antibodies is ~9.3 μg (~0.37 mg/kg dose in 25 g mouse, molar mass of fentanyl = 336.47 g/mol). Indeed, immunized mice remained partially protected even up to 0.50 mg/kg dose, that is, ~12.5 μg fentanyl (~50% MPE, Figure 4B). The potency of fentanyl is much higher in humans than in rodents. While approximately 2 mg fentanyl is considered deadly in humans[60] (i.e. ~0.029 mg/kg assuming 70 kg average human), mice have a fentanyl 50% lethal dose (LD_{50}) value of ~4 mg/kg in male Swiss Webster mice.[37] In our present work, at the 4 mg/kg cumulative dose, all immunized mice survived (Figure 6C). Unvaccinated control mice only received a maximum cumulative dose of 1 mg/kg. Bremer et al.[37] also reported that immunization using an anti-fentanyl vaccine can protect mice from fatal overdose. Taken together, these results suggest that active vaccination is a potential prophylactic to prevent fatal overdose due to fentanyl.

An effective vaccine to fentanyl should be able to raise antibodies that could also cross-react with fentanyl analogues. In this study, we tested the ability of the antisera to bind the following drugs (given are their potencies relative to fentanyl):[61,62] cyclopropyl fentanyl (∼3-fold), furanyl fentanyl (∼7-fold), *para*-fluorofentanyl (∼0.30-fold), *cis*-3-methylfentanyl (∼20-fold), and carfentanil (∼30 to 100-fold). Many deaths have been reported involving these analogues.[9,10,63−66] We found that immunization with TT−*para*-AmFenHap induced IgG capable of binding these analogues (Figure 4). We also obtained the relative antibody binding site concentrations for these drugs (1.44 to 18.84 μM, Table 1). These values can be used to estimate the relative concentration of drug-specific IgG under three assumptions: (1) the relative binding sites calculated from eq 5 correspond to the actual number of binding sites in IgG molecules on a molar basis; (2) the average molecular weight of IgG is 150,000; and (3) the stoichiometry is 1:2 (antibody/binding site). Using these assumptions, the calculated relative IgG concentrations were 1.18 ± 0.07 mg/mL (cyclopropyl fentanyl), 1.41 ± 0.1 mg/mL (furanyl fentanyl), 0.97 ± 0.09 mg/mL (*para*-fluorofentanyl), and 0.11 ± 0.01 mg/mL (carfentanil). These results, along with the nanomolar antibody affinities to these drugs ($K_d = 0.36$ to 4.66 nM) suggest that immunization may be effective in inducing antibodies that could sequester fentanyl analogues in the blood *in vivo*. According to Pearson et al. (2015), the postmortem blood concentrations of fentanyl are about 3 μg/L (∼8.9 nM) to 18 μg/L (∼53.5 nM).[67] The [Ab] values we obtained are >200-fold higher than these clinically relevant concentrations. Our on-going efforts are geared toward testing of vaccine efficacy against these fentanyl analogues in animals.

The [Ab] data presented above should be interpreted judiciously because they were expressed relative to K_d; and they may not necessarily equate to absolute IgG concentrations. For example, the above calculations indicated that the fentanyl-specific IgG binding site concentration was ∼10-fold higher than that of carfentanil. This can be interpreted in terms of antibody affinity rather than absolute concentration. The hapten-specific IgG in sera had a higher affinity to fentanyl than to carfentanil (∼8-fold difference, Table 1); this implied that at equilibrium, fentanyl would occupy a larger fraction of all anti-hapten IgG binding sites available than carfentanil would (other factors being equal). The [Ab] values reported above corresponded to this relative number of available binding sites for specified drugs. This underscored the need to account for K_d values of vaccine-induced IgG to its target antigen when developing an immunotherapeutic against opioids. Moreover, the measurement of absolute IgG concentrations using standard ELISA is limited by the commercially available monoclonal antibodies against the target opioids. Taken together, these results suggested that [Ab] values may serve as a relevant measure of effective IgG concentrations *in vivo*.

Chemical substituents at crucial sites of the parent fentanyl drug modulate the strength of antibody−antigen binding. We found that substitutions at *N*-alkyl group contributed minimal perturbation to binding (furanyl fentanyl and cyclopropyl fentanyl), but subtle modification at the piperidine and terminal phenyl ring (rings *b* and *c*, respectively, in Figure 1) resulted in drastic effects for IgG binding [carfentanil, *para*-fluorofentanyl, and (±)-*cis*-3-methylfentanyl] (Figure 4). Molecular structures play a role in antibody−antigen interactions.[68] To rationalize serum binding results, we looked at optimized space-filling models of these compounds (Figure 7). Using fentanyl as reference (Figure 7B), it was apparent that most structural features had a similar orientation across these analogues, except two—the tilting of phenyl ring *c* with respect to the amide oxygen in carfentanil and the slight distortion of oxygen with respect to phenyl ring *a* in (±)-*cis*-3-methyl fentanyl. Their different orientations may have impacted the interaction of these analogues with the IgG binding pockets.

In the case of *para*-fluorofentanyl, the substitution of fluorine in phenyl ring *a* resulted in weaker binding compared to fentanyl at the same serum dilution (Figure 4A,E), which suggests that the addition of fluorine in this ring weakens the binding to IgG. We also explored the importance of the phenyl ring *c* in antibody−antigen binding using norfentanyl (an inactive metabolite of fentanyl) where ring *c* is absent. The deletion of this phenyl ring attenuated but did not completely abolish its serum binding property (Supporting Information Figure S15). These results suggest that rings *a*, *b*, and *c* are important for binding, with rings *b* and *c* imparting greater weight. These also imply that immunization has "trained" the immune system to recognize rings *a*, *b*, and *c* as crucial epitopes and generated IgG directed toward these epitopes. These findings are consistent with the facial recognition hypothesis of Matyas et al.[53] and agree with the work of Hwang et al.[55] where polyclonal sera (from mice immunized with a fentanyl vaccine) were found to have >10-fold lower affinity to remifentanil ($IC_{50} = 1$ μM) compared to fentanyl ($IC_{50} = 71$ nM). Remifentanil is a fentanyl analogue where ring *c* is replaced by an ester group (−COOCH$_3$). Guided by these results, we hypothesized that the hapten-binding IgG paratope may be composed of pockets that could accommodate rings *a* and *c* through hydrophobic interactions and that the orientation of *c* would dictate the strength of binding. Efforts in our laboratory are underway to explore this hypothesis. Together, these results underline the importance of hapten design to induce broad specificity IgG against opioids.

One important consideration in developing a vaccine against opioids is the non-cross reactivity with opioid abuse pharmacotherapeutics. Using ED and LC−MS/MS, we demonstrated that antibodies induced by the vaccine did not bind naltrexone, buprenorphine, and naloxone. This is not surprising given that their molecules are structurally dissimilar to fentanyl (Figure 7C). Although methadone shares a similar scaffold with fentanyl, their 3D structures are distinctly different (Figure 7C) and may explain why vaccine-induced antibodies did not bind methadone. Bremer et al.[37] reported the same observation. *In vivo*, Raleigh et al.[36] demonstrated that administration of an anti-fentanyl vaccine did not interfere with the therapeutic use of naloxone. Naloxone is used clinically to reverse opioid-induced respiratory depression in overdose cases, while methadone, buprenorphine, and naltrexone are used to manage opioid addiction.[18] Because recovering substance abusers who suddenly halt or begin to taper medications are among the most vulnerable population to opioid overdose,[20] prophylactic immunization may offer them an additional layer of protection. Taken together, these findings emphasize that active immunization and pharmacotherapeutics could be used in combination to combat opioid use disorders.

The present study has some noteworthy limitations. First, the effect of sex difference on the immunogenicity and efficacy of the vaccine was not evaluated in the present study. It has

been well documented that sex differences[69,70] could influence the resulting immunogenicity and efficacy of vaccines to substance abuse. Second, while serum binding experiments demonstrated that the sera from immunized mice did not sequester the drugs used for opioid management therapy (methadone, buprenorphine, naltrexone, and naloxone), it will be necessary to test these drugs *in vivo*.[36,37] Third, a thorough pharmacology—toxicology study following the current Good Laboratory Practices (cGLP) needs to be performed to evaluate the overall safety of the proposed fentanyl vaccine, this is typically carried-out prior to a phase 1 clinical trial. Finally, the present study focused only on the attenuation of the antinociceptive effects of fentanyl. Toward a holistic vaccine against fentanyl and analogues, the vaccine described here will need to be evaluated in terms of its ability to reverse respiratory depression.[34,36]

CONCLUSIONS

We described herein a novel vaccine formulation against fentanyl composed of a novel fentanyl surrogate, a safe and immunogenic carrier protein (TT), and a potent liposomal adjuvant (ALF43A). Immunization in mice generated high hapten-specific antibody titers which strongly bound fentanyl and relevant analogues in serum but not drugs used for opioid abuse management. Antinociceptive effects of fentanyl in mice were blunted by immunization. Taken together, this work highlights the potential of TT—*para*-AmFenHap/ALF43A as a practical and efficacious vaccine that can be easily translated to humans to combat fentanyl intoxication and overdose amid the on-going opioid epidemic.

ASSOCIATED CONTENT

Ⓢ Supporting Information

The Supporting Information is available free of charge at https://pubs.acs.org/doi/10.1021/acs.molpharmaceut.0c00497.

> Supplementary methods, MALDI-TOF MS spectra, IC$_{50}$ values and inhibition curves, anti-TT ELISA, dilution curves, NMR spectra, and norfentanyl serum binding curve (PDF)

AUTHOR INFORMATION

Corresponding Author

Gary R. Matyas — *Laboratory of Adjuvant and Antigen Research, U.S. Military HIV Research Program, Walter Reed Army Institute of Research, Silver Spring, Maryland 20910, United States;* ⓞ orcid.org/0000-0002-2074-2373; Phone: 301-319-9973; Email: gmatyas@hivresearch.org; Fax: 301-319-7518

Authors

Rodell C. Barrientos — *Laboratory of Adjuvant and Antigen Research, U.S. Military HIV Research Program, Walter Reed Army Institute of Research, Silver Spring, Maryland 20910, United States; U.S. Military HIV Research Program, Henry M. Jackson Foundation for the Advancement of Military Medicine, Bethesda, Maryland 20817, United States;* ⓞ orcid.org/0000-0002-6006-5047

Eric W. Bow — *Drug Design and Synthesis Section, Molecular Targets and Medications Discovery Branch, Intramural Research Program, National Institute on Drug Abuse and the National Institute on Alcohol Abuse and Alcoholism,*

Department of Health and Human Services, National Institutes of Health, Bethesda, Maryland 20892-3373, United States

Connor Whalen — *Laboratory of Adjuvant and Antigen Research, U.S. Military HIV Research Program, Walter Reed Army Institute of Research, Silver Spring, Maryland 20910, United States*

Oscar B. Torres — *Laboratory of Adjuvant and Antigen Research, U.S. Military HIV Research Program, Walter Reed Army Institute of Research, Silver Spring, Maryland 20910, United States; U.S. Military HIV Research Program, Henry M. Jackson Foundation for the Advancement of Military Medicine, Bethesda, Maryland 20817, United States*

Agnieszka Sulima — *Drug Design and Synthesis Section, Molecular Targets and Medications Discovery Branch, Intramural Research Program, National Institute on Drug Abuse and the National Institute on Alcohol Abuse and Alcoholism, Department of Health and Human Services, National Institutes of Health, Bethesda, Maryland 20892-3373, United States*

Zoltan Beck — *Laboratory of Adjuvant and Antigen Research, U.S. Military HIV Research Program, Walter Reed Army Institute of Research, Silver Spring, Maryland 20910, United States; U.S. Military HIV Research Program, Henry M. Jackson Foundation for the Advancement of Military Medicine, Bethesda, Maryland 20817, United States*

Arthur E. Jacobson — *Drug Design and Synthesis Section, Molecular Targets and Medications Discovery Branch, Intramural Research Program, National Institute on Drug Abuse and the National Institute on Alcohol Abuse and Alcoholism, Department of Health and Human Services, National Institutes of Health, Bethesda, Maryland 20892-3373, United States*

Kenner C. Rice — *Drug Design and Synthesis Section, Molecular Targets and Medications Discovery Branch, Intramural Research Program, National Institute on Drug Abuse and the National Institute on Alcohol Abuse and Alcoholism, Department of Health and Human Services, National Institutes of Health, Bethesda, Maryland 20892-3373, United States*

Complete contact information is available at:
https://pubs.acs.org/10.1021/acs.molpharmaceut.0c00497

Notes

ACKNOWLEDGMENTS

■ ABBREVIATIONS

[Ab], relative antibody binding site concentration; ALF43A, army liposome formulation with 43% cholesterol on aluminum hydroxide; BSA, bovine serum albumin; DMPC, 1,2-dimyristoyl-*sn*-glycero-3-phosphocholine; DMPG, 1,2-dimyristoyl-*sn*-glycero-3-phosphoglycerol; 3D-PHAD, monophosphoryl 3-deacyl lipid A; ED_{50}, 50% effective dose; ELISA, enzyme-linked immunosorbent assay; IC_{50}, 50% inhibitory concentration; K_d, dissociation constant; MALDI-TOF MS, matrix-assisted laser desorption/ionization time-of-flight mass spectrometry; LC–MS/MS, liquid chromatography tandem mass spectrometry; LD_{50}, 50% lethal dose; MPE, maximum potential effect; MWCO, molecular weight cutoff; *para*-AmFenHap, *N*-phenyl-*N*-(1-(4-(3-(tritylthio)propanamido)-phenethyl)piperidin-4-yl)propionamide; s.c., subcutaneous; i.m., intramuscular; SM(PEG)$_2$, succinimidyl-[(*N*-maleimido-propionamido)-diethylene glycol]ester; TT, tetanus toxoid

■ REFERENCES

(1) Socías, M. E.; Wood, E. Epidemic of deaths from fentanyl overdose. *Br. Med. J.* **2017**, *358*, j4355.

(2) Volkow, N. D.; Collins, F. S. The Role of Science in Addressing the Opioid Crisis. *N. Engl. J. Med.* **2017**, *377*, 391−394.

(3) Han, Y.; Yan, W.; Zheng, Y.; Khan, M. Z.; Yuan, K.; Lu, L. The rising crisis of illicit fentanyl use, overdose, and potential therapeutic strategies. *Transl. Psychiatry* **2019**, *9*, 282.

(4) Gostin, L. O.; Hodge, J. G., Jr.; Noe, S. A. Reframing the Opioid Epidemic as a National Emergency. *JAMA, J. Am. Med. Assoc.* **2017**, *318*, 1539−1540.

(5) Wilson, N.; Kariisa, M.; Seth, P.; Smith, H.; Davis, N. L. Drug and Opioid-Involved Overdose Deaths—United States, 2017−2018. *Morb. Mortal. Wkly. Rep.* **2020**, *69*, 290−297.

(6) Armenian, P.; Vo, K. T.; Barr-Walker, J.; Lynch, K. L. Fentanyl, fentanyl analogs and novel synthetic opioids: A comprehensive review. *Neuropharmacology* **2018**, *134*, 121−132.

(7) Comer, S. D.; Cahill, C. M. Fentanyl: Receptor pharmacology, abuse potential, and implications for treatment. *Neurosci. Biobehav. Rev.* **2019**, *106*, 49−57.

(8) Bryce, P.; Taylor, J.; Caulkins, J.; Kilmer, B.; Reuter, P.; Stein, B. *The Future of Fentanyl and Other Synthetic Opioids*; RAND Corporation: Santa Monica, CA, 2019.

(9) Drummer, O. H. Fatalities caused by novel opioids: a review. *Forensic Sci. Prog.* **2018**, *4*, 95−110.

(10) Concheiro, M.; Chesser, R.; Pardi, J.; Cooper, G. Postmortem Toxicology of New Synthetic Opioids. *Front. Pharmacol.* **2018**, *9*, 1210.

(11) Dembek, Z. F.; Chekol, T.; Wu, A. The Opioid Epidemic: Challenge to Military Medicine and National Security. *Mil. Med.* **2020**, *185*, e662−e667.

(12) Caves, J. P. J. Fentanyl as a Chemical Weapon. *CSWMD Proceedings*; National Defense University Press: 2019; pp 1−5.

(13) Talu, A.; Rajaleid, K.; Abel-Ollo, K.; Rüütel, K.; Rahu, M.; Rhodes, T.; Platt, L.; Bobrova, N.; Uusküla, A. HIV infection and risk behaviour of primary fentanyl and amphetamine injectors in Tallinn, Estonia: implications for intervention. *Int. J. Drug Policy* **2010**, *21*, 56−63.

(14) Lambdin, B. H.; Bluthenthal, R. N.; Zibbell, J. E.; Wenger, L.; Simpson, K.; Kral, A. H. Associations between perceived illicit fentanyl use and infectious disease risks among people who inject drugs. *Int. J. Drug Policy* **2019**, *74*, 299−304.

(15) *World Drug Report*. https://wdr.unodc.org/wdr2019/en/exsum.html (June 19, 2020).

(16) Center for Disease Control and Prevention. Estimated HIV incidence and prevalence in the United States, 2014−2018. *HIV Surveillance Supplemental Report*, 2020; Vol. 25 (1).

(17) Florence, C. S.; Zhou, C.; Luo, F.; Xu, L. The Economic Burden of Prescription Opioid Overdose, Abuse, and Dependence in the United States, 2013. *Med. Care* **2016**, *54*, 901−906.

(18) Blanco, C.; Volkow, N. D. Management of opioid use disorder in the USA: present status and future directions. *Lancet* **2019**, *393*, 1760−1772.

(19) Hoffman, K. A.; Ponce Terashima, J.; McCarty, D. Opioid use disorder and treatment: challenges and opportunities. *BMC Health Serv. Res.* **2019**, *19*, 884.

(20) Fenton, J. J.; Agnoli, A. L.; Xing, G.; Hang, L.; Altan, A. E.; Tancredi, D. J.; Jerant, A.; Magnan, E. Trends and Rapidity of Dose Tapering Among Patients Prescribed Long-term Opioid Therapy, 2008-2017. *JAMA Netw. Open* **2019**, *2*, e1916271.

(21) Rzasa Lynn, R.; Galinkin, J. Naloxone dosage for opioid reversal: current evidence and clinical implications. *Ther. Adv. Drug Saf.* **2018**, *9*, 63−88.

(22) Moss, R. B.; Carlo, D. J. Higher doses of naloxone are needed in the synthetic opioid era. *Subst. Abuse Treat. Prev. Policy* **2019**, *14*, 6.

(23) Levine, R.; Veliz, S.; Singer, D. Wooden chest syndrome: Beware of opioid antagonists, not just agonists. *Am. J. Emerg. Med.* **2020**, *38*, 411.e5−411.e6.

(24) Olson, M. E.; Janda, K. D. Vaccines to combat the opioid crisis: Vaccines that prevent opioids and other substances of abuse from entering the brain could effectively treat addiction and abuse. *EMBO Rep.* **2018**, *19*, 5−9.

(25) Bremer, P. T.; Janda, K. D. Conjugate Vaccine Immunotherapy for Substance Use Disorder. *Pharmacol. Rev.* **2017**, *69*, 298−315.

(26) Baehr, C.; Pravetoni, M. Vaccines to treat opioid use disorders and to reduce opioid overdoses. *Neuropsychopharmacology* **2019**, *44*, 217−218.

(27) Torres, O. B.; Alving, C. R.; Jacobson, A. E.; Rice, K. C.; Matyas, G. R. Practical Considerations for the Development of Vaccines Against Drugs of Abuse. In *Biologics to Treat Substance Use Disorders: Vaccines, Monoclonal Antibodies, and Enzymes*; Montoya, I. D., Ed.; Springer International Publishing: Cham, 2016; pp 397−424.

(28) Goniewicz, M. L.; Delijewski, M. Nicotine vaccines to treat tobacco dependence. *Hum. Vaccines Immunother.* **2013**, *9*, 13−25.

(29) Nguyen, J. D.; Bremer, P. T.; Hwang, C. S.; Vandewater, S. A.; Collins, K. C.; Creehan, K. M.; Janda, K. D.; Taffe, M. A. Effective active vaccination against methamphetamine in female rats. *Drug Alcohol Depend.* **2017**, *175*, 179−186.

(30) Kinsey, B. M.; Kosten, T. R.; Orson, F. M. Anti-cocaine vaccine development. *Expert Rev. Vaccines* **2010**, *9*, 1109−1114.

(31) Raleigh, M. D.; Peterson, S. J.; Laudenbach, M.; Baruffaldi, F.; Carroll, F. I.; Comer, S. D.; Navarro, H. A.; Langston, T. L.; Runyon, S. P.; Winston, S.; Pravetoni, M.; Pentel, P. R. Safety and efficacy of an oxycodone vaccine: Addressing some of the unique considerations posed by opioid abuse. *PLoS One* **2017**, *12*, e0184876.

(32) Sulima, A.; Jalah, R.; Antoline, J. F. G.; Torres, O. B.; Imler, G. H.; Deschamps, J. R.; Beck, Z.; Alving, C. R.; Jacobson, A. E.; Rice, K. C.; Matyas, G. R. A Stable Heroin Analogue That Can Serve as a Vaccine Hapten to Induce Antibodies That Block the Effects of Heroin and Its Metabolites in Rodents and That Cross-React Immunologically with Related Drugs of Abuse. *J. Med. Chem.* **2018**, *61*, 329−343.

(33) Hwang, C. S.; Smith, L. C.; Natori, Y.; Ellis, B.; Zhou, B.; Janda, K. D. Efficacious Vaccine against Heroin Contaminated with Fentanyl. *ACS Chem. Neurosci.* **2018**, *9*, 1269−1275.

(34) Townsend, E. A.; Blake, S.; Faunce, K. E.; Hwang, C. S.; Natori, Y.; Zhou, B.; Bremer, P. T.; Janda, K. D.; Banks, M. L. Conjugate vaccine produces long-lasting attenuation of fentanyl vs. food choice and blocks expression of opioid withdrawal-induced increases in fentanyl choice in rats. *Neuropsychopharmacology* **2019**, *44*, 1681−1689.

(35) Tenney, R. D.; Blake, S.; Bremer, P. T.; Zhou, B.; Hwang, C. S.; Poklis, J. L.; Janda, K. D.; Banks, M. L. Vaccine blunts fentanyl potency in male rhesus monkeys. *Neuropharmacology* **2019**, *158*, 107730.

(36) Raleigh, M. D.; Baruffaldi, F.; Peterson, S. J.; Le Naour, M.; Harmon, T. M.; Vigliaturo, J. R.; Pentel, P. R.; Pravetoni, M. A Fentanyl Vaccine Alters Fentanyl Distribution and Protects against Fentanyl-Induced Effects in Mice and Rats. *J. Pharmacol. Exp. Ther.* **2019**, *368*, 282−291.

(37) Bremer, P. T.; Kimishima, A.; Schlosburg, J. E.; Zhou, B.; Collins, K. C.; Janda, K. D. Combatting Synthetic Designer Opioids: A Conjugate Vaccine Ablates Lethal Doses of Fentanyl Class Drugs. *Angew. Chem., Int. Ed.* **2016**, *55*, 3772−3775.

(38) Townsend, E. A.; Bremer, P. T.; Faunce, K. E.; Negus, S. S.; Jaster, A. M.; Robinson, H. L.; Janda, K. D.; Banks, M. L. Evaluation of a Dual Fentanyl/Heroin Vaccine on the Antinociceptive and Reinforcing Effects of a Fentanyl/Heroin Mixture in Male and Female Rats. *ACS Chem. Neurosci.* **2020**, *11*, 1300−1310.

(39) Raleigh, M. D.; Laudenbach, M.; Baruffaldi, F.; Peterson, S. J.; Roslawski, M. J.; Birnbaum, A. K.; Carroll, F. I.; Runyon, S. P.; Winston, S.; Pentel, P. R.; Pravetoni, M. Opioid Dose- and Route-Dependent Efficacy of Oxycodone and Heroin Vaccines in Rats. *J. Pharmacol. Exp. Ther.* **2018**, *365*, 346−353.

(40) Alving, C. R.; Peachman, K. K.; Matyas, G. R.; Rao, M.; Beck, Z. Army Liposome Formulation (ALF) family of vaccine adjuvants. *Expert Rev. Vaccines* **2020**, *19*, 279−292.

(41) Matyas, G. R.; Muderhwa, J. M.; Alving, C. R. Oil-in-water liposomal emulsions for vaccine delivery. *Methods Enzymol.* **2003**, *373*, 34−50.

(42) Matyas, G. R.; Mayorov, A. V.; Rice, K. C.; Jacobson, A. E.; Cheng, K.; Iyer, M. R.; Li, F.; Beck, Z.; Janda, K. D.; Alving, C. R. Liposomes containing monophosphoryl lipid A: a potent adjuvant system for inducing antibodies to heroin hapten analogs. *Vaccine* **2013**, *31*, 2804−2810.

(43) Burke, T. R., Jr.; Bajwa, B. S.; Jacobson, A. E.; Rice, K. C.; Streaty, R. A.; Klee, W. A. Probes for narcotic receptor mediated phenomena. 7. Synthesis and pharmacological properties of irreversible ligands specific for mu or delta opiate receptors. *J. Med. Chem.* **1984**, *27*, 1570−1574.

(44) Torres, O. B.; Jalah, R.; Rice, K. C.; Li, F.; Antoline, J. F. G.; Iyer, M. R.; Jacobson, A. E.; Boutaghou, M. N.; Alving, C. R.; Matyas, G. R. Characterization and optimization of heroin hapten-BSA conjugates: method development for the synthesis of reproducible hapten-based vaccines. *Anal. Bioanal. Chem.* **2014**, *406*, 5927−5937.

(45) Torres, O. B.; Alving, C. R.; Matyas, G. R. Synthesis of Hapten-Protein Conjugate Vaccines with Reproducible Hapten Densities. *Methods Mol. Biol.* **2016**, *1403*, 695−710.

(46) Beck, Z.; Torres, O. B.; Matyas, G. R.; Lanar, D. E.; Alving, C. R. Immune response to antigen adsorbed to aluminum hydroxide particles: Effects of co-adsorption of ALF or ALFQ adjuvant to the aluminum-antigen complex. *J. Controlled Release* **2018**, *275*, 12−19.

(47) *Guide for the Care and Use of Laboratory Animals*; National Academies Press (US), National Academy of Sciences: Washington (DC), 2011.

(48) Jalah, R.; Torres, O. B.; Mayorov, A. V.; Li, F.; Antoline, J. F. G.; Jacobson, A. E.; Rice, K. C.; Deschamps, J. R.; Beck, Z.; Alving, C. R.; Matyas, G. R. Efficacy, but not antibody titer or affinity, of a heroin hapten conjugate vaccine correlates with increasing hapten densities on tetanus toxoid, but not on CRM197 carriers. *Bioconjugate Chem.* **2015**, *26*, 1041−1053.

(49) Le Bars, D.; Gozariu, M.; Cadden, S. W. Animal models of nociception. *Pharmacol. Rev.* **2001**, *53*, 597−652.

(50) Torres, O. B.; Antoline, J. F. G.; Li, F.; Jalah, R.; Jacobson, A. E.; Rice, K. C.; Alving, C. R.; Matyas, G. R. A simple nonradioactive method for the determination of the binding affinities of antibodies induced by hapten bioconjugates for drugs of abuse. *Anal. Bioanal. Chem.* **2016**, *408*, 1191−1204.

(51) Müller, R. Determination of affinity and specificity of anti-hapten antibodies by competitive radioimmunoassay. *Methods Enzymol.* **1983**, *92*, 589−601.

(52) Motulsky, H.; Christopoulos, A. *Fitting Models to Biological Data Using Linear and Nonlinear Regression*; GraphPad Software Inc.: San Diego, CA, 2003.

(53) Matyas, G. R.; Rice, K. C.; Cheng, K.; Li, F.; Antoline, J. F. G.; Iyer, M. R.; Jacobson, A. E.; Mayorov, A. V.; Beck, Z.; Torres, O. B.; Alving, C. R. Facial recognition of heroin vaccine opiates: type 1 cross-reactivities of antibodies induced by hydrolytically stable haptenic surrogates of heroin, 6-acetylmorphine, and morphine. *Vaccine* **2014**, *32*, 1473−1479.

(54) Pravetoni, M.; Vervacke, J. S.; Distefano, M. D.; Tucker, A. M.; Laudenbach, M.; Pentel, P. R. Effect of currently approved carriers and adjuvants on the pre-clinical efficacy of a conjugate vaccine against oxycodone in mice and rats. *PLoS One* **2014**, *9*, e96547.

(55) Hwang, C. S.; Smith, L. C.; Natori, Y.; Ellis, B.; Zhou, B.; Janda, K. D. Improved Admixture Vaccine of Fentanyl and Heroin Hapten Immunoconjugates: Antinociceptive Evaluation of Fentanyl-Contaminated Heroin. *ACS Omega* **2018**, *3*, 11537−11543.

(56) TDVAX. https://www.fda.gov/vaccines-blood-biologics/vaccines/tdvax (accessed on Feb 8, 2020).

(57) Natori, Y.; Hwang, C. S.; Lin, L.; Smith, L. C.; Zhou, B.; Janda, K. D. A chemically contiguous hapten approach for a heroin-fentanyl vaccine. *Beilstein J. Org. Chem.* **2019**, *15*, 1020−1031.

(58) Barrot, M. Tests and models of nociception and pain in rodents. *Neuroscience* **2012**, *211*, 39−50.

(59) Smith, L. C.; Bremer, P. T.; Hwang, C. S.; Zhou, B.; Ellis, B.; Hixon, M. S.; Janda, K. D. Monoclonal Antibodies for Combating Synthetic Opioid Intoxication. *J. Am. Chem. Soc.* **2019**, *141*, 10489−10503.

(60) Fentanyl Drug Profile. http://www.emcdda.europa.eu/publications/drug-profiles/fentanyl (accessed on Feb 8, 2020).

(61) Wilde, M.; Pichini, S.; Pacifici, R.; Tagliabracci, A.; Busardò, F. P.; Auwärter, V.; Solimini, R. Metabolic Pathways and Potencies of New Fentanyl Analogs. *Front. Pharmacol.* **2019**, *10*, 238.

(62) Higashikawa, Y.; Suzuki, S. Studies on 1-(2-phenethyl)-4-(N-propionylanilino)piperidine (fentanyl) and its related compounds. VI. Structure-analgesic activity relationship for fentanyl, methyl-substituted fentanyls and other analogues. *Forensic Toxicol.* **2008**, *26*, 1−5.

(63) Fogarty, M. F.; Papsun, D. M.; Logan, B. K. Analysis of Fentanyl and 18 Novel Fentanyl Analogs and Metabolites by LC-MS-MS, and report of Fatalities Associated with Methoxyacetylfentanyl and Cyclopropylfentanyl. *J. Anal. Toxicol.* **2018**, *42*, 592−604.

(64) Mohr, A. L. A.; Friscia, M.; Papsun, D.; Kacinko, S. L.; Buzby, D.; Logan, B. K. Analysis of Novel Synthetic Opioids U-47700, U-50488 and Furanyl Fentanyl by LC-MS/MS in Postmortem Casework. *J. Anal. Toxicol.* **2016**, *40*, 709−717.

(65) Sofalvi, S.; Schueler, H. E.; Lavins, E. S.; Kaspar, C. K.; Brooker, I. T.; Mazzola, C. D.; Dolinak, D.; Gilson, T. P.; Perch, S. An LC-MS-MS Method for the Analysis of Carfentanil, 3-Methylfentanyl, 2-Furanyl Fentanyl, Acetyl Fentanyl, Fentanyl and Norfentanyl in Postmortem and Impaired-Driving Cases. *J. Anal. Toxicol.* **2017**, *41*, 473−483.

(66) Guerrieri, D.; Rapp, E.; Roman, M.; Druid, H.; Kronstrand, R. Postmortem and Toxicological Findings in a Series of Furanylfentanyl-Related Deaths. *J. Anal. Toxicol.* **2017**, *41*, 242−249.

(67) Pearson, J.; Poklis, J.; Poklis, A.; Wolf, C.; Mainland, M.; Hair, L.; Devers, K.; Chrostowski, L.; Arbefeville, E.; Merves, M. Postmortem Toxicology Findings of Acetyl Fentanyl, Fentanyl, and Morphine in Heroin Fatalities in Tampa, Florida. *Acad Forensic Pathol.* **2015**, *5*, 676−689.

(68) Sela-Culang, I.; Kunik, V.; Ofran, Y. The structural basis of antibody-antigen recognition. *Front. Immunol.* **2013**, *4*, 302.

(69) Hwang, C. S.; Smith, L. C.; Wenthur, C. J.; Ellis, B.; Zhou, B.; Janda, K. D. Heroin vaccine: Using titer, affinity, and antinociception as metrics when examining sex and strain differences. *Vaccine* **2019**, *37*, 4155−4163.

(70) Cicero, T. J.; Nock, B.; Meyer, E. R. Sex-related differences in morphine's antinociceptive activity: relationship to serum and brain morphine concentrations. *J. Pharmacol. Exp. Ther.* **1997**, *282*, 939−944.